Performance Evaluation of Filterbank Multicarrier Systems in an Underwater Acoustic Channel

Mohammud J. Bocus, Angela Doufexi, and Dimitris Agrafiotis
Department of Electrical and Electronic Engineering, University of Bristol, BS8 1UB, UK.

***Abstract*— This paper examines the performance of filter bank multicarrier (FBMC) systems for underwater acoustic communications. We evaluate the performance of Filtered Multitone (FMT) and Orthogonal Frequency Division Multiplexing-Offset Quadrature Amplitude Modulation (OFDM-OQAM) and compare it to that of traditional OFDM. OFDM-OQAM is found to be the most suitable multicarrier technique that can be applied to underwater acoustic communications as it achieves maximum bandwidth efficiency and provides a higher bit rate than its OFDM counterpart due to the absence of a cyclic prefix (CP). We also present a bit error rate (BER) performance evaluation of coded and un-coded OFDM-OQAM for both horizontally and vertically configured acoustic channels.**

I. Introduction

Orthogonal Frequency Division Multiplexing (OFDM) is currently the most commonly used multicarrier technique due to its robustness against inter symbol interference (ISI) - caused by delay spread in frequency selective channels-, better bandwidth efficiency compared to traditional FDM systems and simple frequency domain equalization. The use of a cyclic prefix (CP) is a key element in an OFDM system, however its usage represents wastage of useful bandwidth that could have been otherwise used for data transmission. Additionally OFDM exhibits out-of-band power leakage and sensitivity to frequency dispersion. A small frequency offset can cause the subcarriers to lose their orthogonality leading to inter carrier interference (ICI). In the case of underwater acoustic (UWA) channels, the channel impulse response (CIR) can span hundreds of milliseconds and if OFDM is used, the CP duration must at least match the length of the CIR. The longer symbol duration (hence smaller subcarrier spacing) may result in poor receiver performance since UWA channels also exhibit significant dispersion which leads to ISI [1].

OFDM has been largely investigated for UWA transmission because the bandwidth available in such a channel is very limited. A small number of studies have focused on underwater wireless video transmission and have shown that acceptable bit rates can be achieved using OFDM, promoting the case of real-time video transmission over a specific range [2]–[4].

In filter bank multicarrier (FBMC) transmission where CP is not used, robust performance in channels characterized by both time and frequency dispersions (doubly-dispersive) can still be achieved through the use of suitable pulse shaping filters such as Isotropic Orthogonal Transform Algorithm (IOTA) [5] and Hermite function based prototype filters [6].

Recent studies have addressed the feasibility of FBMC systems for UWA communication [7]–[9]. For instance in [7] the authors proposed to use a Filtered Multitone (FMT) system with relatively wideband subcarriers. This work focused on a channel-estimation based Decision Feedback (DFE) equalization. Their design required a multi-tap equalizer per subcarrier. Simulation results showed that FMT may outperform OFDM in the presence of channel variation but the experimental data were not conclusive in this respect.

FMT was also investigated in [8] where a prototype filter with hexagonal lattice structure was proposed to address doubly-dispersive channels. The filter is essentially a more robust version of the Haas and Belfiore [6] method which is based on Hermite functions. FMT was chosen due to its simpler structure and the fact that it is easily applicable to Multiple-Input-Multiple-Output (MIMO) systems. In this modified FMT system, the subcarriers were allowed to overlap to a smaller extent. In terms of signal-to-interference ratio (SIR), the modified FMT system exhibited better performance than OFDM and conventional non-overlapping FMT in a high mobility environment. Each subcarrier was assumed to experience flat fading and therefore the channel at each subcarrier was estimated as a complex valued gain using pilot symbols. Hence a one-tap equalizer was used in this work.

Cosine Multitone (CMT) was investigated for UWA communication in [9]. The work focused on Doppler compensation using a low-complexity algorithm based on frequency spreading. The choice of CMT was based on the fact that it can achieve a bandwidth efficiency of 100%. Frequency spreading multi-tap equalization was used in order to have a wider bandwidth for each subcarrier and achieve a more precise equalization. A channel that introduced only a time scaling to the transmit signal was considered. The SIR of a 64-subcarrier system was analyzed by varying the Doppler scaling factor α. It was shown that for α values ranging from 0 to 0.05, the SIR was fairly constant at about 65 dB. For negative values, the SIR started to degrade to about 56 dB which can be considered to be a negligible degradation.

In this paper, we first examine the bit error rate (BER) performance of OFDM-offset quadrature amplitude modulation (OQAM) and FMT in additive white Gaussian noise (AWGN) and Rayleigh channels. Our simulation results show that both mutlicarrier systems can achieve similar performance to OFDM, with OFDM-OQAM being better suited to bandwidth-limited UWA channels as it offers better bandwidth efficiency. We subsequently perform simulations of OFDM-OQAM in horizontally and vertically configured acoustic channels where it is shown how with the use of error-correcting codes the

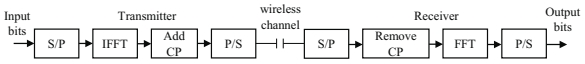

Fig. 1. OFDM basic block diagram

performance of the system can be greatly improved.

The rest of the paper is organized as follows. Section II provides a brief introduction of OFDM and FBMC systems, namely OFDM-OQAM and FMT. Section III describes the typical characteristics of a UWA channel. Section IV presents simulation results of the multicarrier systems in AWGN, Rayleigh fading and horizontally and vertically configured UWA channels. Conclusions are given at the end of this paper.

II. OFDM AND FBMC SYSTEMS

A. OFDM

The general block diagram of an OFDM system is shown in Fig. 1. At the transmitter an input bitstream is mapped to symbols using QAM modulation followed by serial-to-parallel (S/P) conversion. For M subcarriers the modulated symbols can be represented as $X[0], X[1], \cdots, X[M-1]$. N-point inverse Fast Fourier Transform (IFFT) is then applied to the frequency-domain symbol block of length M to yield the time domain OFDM waveform. In order to mitigate ISI between consecutive OFDM symbols, a CP is appended to each of them the length of which is greater than the channel delay spread. The baseband transmitted signal can be represented as follows [10]

$$x[n] = \frac{1}{\sqrt{M}} \sum_{i=0}^{M-1} X[i] e^{j\frac{2\pi}{M}ni}, \quad 0 \le n \le M-1 \qquad (1)$$

where M is the number of subcarriers and $X[i]$ represents the modulated symbol on the ith subcarrier.

At the receiver the reverse process is performed to yield the estimates of the transmitted symbols. Assuming perfect reconstruction, the received signal can be represented as

$$\hat{X}[i] = \frac{1}{\sqrt{M}} \sum_{n=0}^{M-1} x[n] e^{-j\frac{2\pi}{M}ni}, \quad 0 \le i \le M-1 \qquad (2)$$

B. OFDM-OQAM

FBMC-OQAM can be implemented using the frequency-spreading (FS) technique or the polyphase network (PPN) technique. The latter technique reduces the high complexity which is introduced by additional filtering operations at the transmitter and receiver [10]. A polyphase implementation of OFDM-OQAM is illustrated in Fig. 2 [11]. The input bitstream is first mapped to QAM modulated symbols $c_k[l]$ followed by an OQAM pre-processing operation. This consists of a complex-to-real conversion where the real and imaginary part of each QAM symbol is separated by half of a symbol duration. This conversion increases the sampling rate by a factor of 2. The real valued symbols are then multiplied by $\theta_{k,n} = j^{k+n}$ sequence (where n is the sample index at pre-processing output and post-processing input and k is the subcarrier index). This operation makes the adjacent

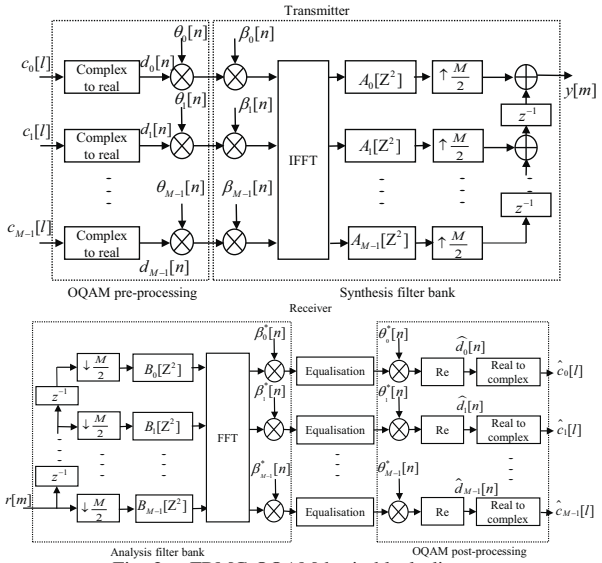

Fig. 2. FBMC-OQAM basic block diagram

subcarriers orthogonal to each other. The transmit signal can be expressed as:

$$y[m] = \sum_{k=0}^{M-1} \sum_{n=-\infty}^{\infty} x_k[n] \beta_k[n] p\left[m - \frac{nM}{2}\right] e^{j\frac{2\pi}{M}km} \qquad (3)$$

where m is the sample index at the synthesis filter bank (SFB) output and the analysis filter bank (AFB) input. $p[m]$ is the prototype filter of length L_p. $\beta_k[n]$ and $x_k[n]$ are given by the following equations:

$$\beta_k[n] = (-1)^{kn} \exp\left(-j\frac{2\pi k}{M}\left(\frac{L_p-1}{2}\right)\right) \qquad (4)$$

$$x_k[n] = d_k[n]\theta_k[n] \qquad (5)$$

where $d_k[n]$ represents the real-valued symbols for subcarrier k. The prototype filter $p[m]$ is shifted in frequency to produce the subchannels which cover the whole bandwidth [12]. The kth synthesis filter can be expressed as

$$g_k[m] = p[m] \exp\left(j\frac{2\pi k}{M}\left(\frac{L_p-1}{2}\right)\right) \qquad (6)$$

where $m = 0, 1, \ldots, L_p - 1$. The length L_p depends on the size of the filter bank (M subcarriers) and the number of OQAM symbol waveforms K that overlap in the time domain as $L_p = KM$ [12]. Assuming perfect reconstruction (PR) (achieved in an ideal transmission channel), the kth analysis filter is a time-reversed and complex-conjugated version of the corresponding synthesis filter which is defined as:

$$f_k[m] = g_k^*[L_p - 1 - m] \qquad (7)$$

However since the wireless channel is not ideal, the prototype filter is designed such that it guarantees near perfect reconstruction (NPR). NPR means that the output signals are approximately delayed versions of the input ones and a small amount of filter bank induced distortion can be tolerated provided they it is smaller compared to the distortion introduced by the channel [13].

The prototype filter can be designed using the frequency

sampling method or window-based technique [12]. In the former method, the impulse response of the filter coefficients are obtained by taking the IFFT of the KM samples from the desired frequency response of the filter. In this work we used the frequency sampling-based finite impulse response (FIR) prototype filter proposed in the PHYDYAS project [11] for the OFDM-OQAM system. The frequency domain coefficients of this filter for an overlapping factor of $K = 4$ are

$$P_0 = 1; P_{\pm 1} = 0.97196; P_{\pm 2} = \sqrt{2}/2; P_{\pm 3} = 0.235147 \quad (8)$$

For this value of K, a highly frequency selective filter is achieved with almost no out of band leakage. The frequency response of the filter is described by the equation:

$$P(f) = \sum_{k=-(K-1)}^{K-1} P_k \frac{\sin\left(\pi\left(f - \frac{k}{MK}\right)MK\right)}{MK\sin\left(\pi\left(f - \frac{k}{MK}\right)\right)} \quad (9)$$

The corresponding impulse response is obtained by taking the IFFT of the frequency response:

$$p[m] = 1 + 2\sum_{k=1}^{K-1}(-1)^k P_k \cos\left(\frac{2\pi k}{MK}m\right),\ p[0] = 0 \quad (10)$$

The term $p[0]$ is included in order to make the total number of coefficients an odd value. By doing so, the filter delay can be adjusted to an integer multiples of the sample period [10].

In OFDM-OQAM, odd (or even) subcarriers are not overlapped. If only QAM symbols were to be used then it would only be possible to employ the alternate subcarriers. This would however reduce the capacity of the system by half. In order to achieve the maximum capacity all subcarriers have to be used and therefore orthogonality is required between adjacent subcarriers [11]. This is why OQAM modulation is used.

Since in OFDM-OQAM the real and imaginary parts of the symbols are transmitted alternatively, equalization has to be performed so that ISI due to the frequency-selective nature of the channel does not occur between the adjacent symbols. If the number of subcarriers in the system is large enough each subcarrier will experience flat-fading and hence a single-tap equalizer per subcarrier will be adequate to remove any distortion. A number of per-subcarrier equalization methods have been proposed in [14] ranging from a classical one-tap approach, frequency sampling, fractionally-spaced Minimum Mean Squared Error (MMSE), simplified MMSE and fractionally-spaced adaptive Least Mean Squared (LMS). Multiband band MMSE equalization is also proposed. Assuming perfect channel estimation, it was shown that the multiband band MMSE equalizer provides the best performance at high signal-to-noise ratio (SNR) values in highly frequency selective channels but it has a higher complexity. This equalization method also outperforms the conventional CP-OFDM.

C. FILTERED MULTITONE

The basic concept behind FMT is that the total bandwidth, B, is divided into M non-overlapping subchannels, where each one has a bandwidth of B/M, hence FMT is not as bandwidth efficient as OFDM-OQAM. In order to achieve almost perfect spectral containment pulse shaping filters are used. Since the number of subcarriers in FMT is usually much less than in OFDM, the subcarrier bandwidth is wider, i.e., a shorter symbol duration. The wide subcarrier bandwidth coupled with the ability to contain the spectrum make FMT very robust against ICI [7]. The block diagram of an FMT transceiver system is shown in Fig. 3 [15]. The filter bank is implemented from the frequency shifted versions of a lowpass prototype filter defined as [15]

$$h_n^{(i)}(n) = \frac{1}{\sqrt{M}} h(n) e^{j2\pi \frac{i}{M} n}, \quad (11)$$

where $n = 0, 1, \ldots, M\gamma - 1$ and $i = 0, 1, \ldots, M-1$, M is the number of subcarriers and γ is the overlapping factor which takes values between 8 and 20. The length of the prototype filter is given by $M\gamma$. $A^{(i)}(k)$ are PSK or QAM symbols which are up-sampled by a factor of M with each symbol being filtered at a rate M/T (where T is the FMT symbol period). The M filtered signals that have been appropriately shifted in frequency are then summed to give the overall transmit signal $x(n)$. Each subcarrier is centered at a frequency $fi = i/T$. The signal at the transmitter output is expressed as

$$x[n] = \sum_{k=-\infty}^{\infty} h(n - kM) \frac{1}{\sqrt{M}} \sum_{i=0}^{M-1} A^{(i)}(k) e^{j2\pi in/M} \quad (12)$$

where the indices k and n denote samples with a period T and T/M respectively. At the receiver, the filters are matched to those of the transmitter, that is $G^i(f) = (H^i(f))^*$. The analysis filter is expressed as

$$g^{(i)}(n) = \frac{1}{\sqrt{M}} h(n-1) e^{j2\pi \frac{i}{M} n}, \quad n = 1, 2, \ldots, M\gamma \quad (13)$$

Hence the output of the ith subchannel is given by

$$\begin{aligned} B^{(i)}(k) &= \sum_{n=1}^{M\gamma} y(kM - n) g^{(i)}(n) \\ &= \frac{1}{\sqrt{M}} \sum_{n=1}^{M\gamma} y(kM - n) h(n-1) e^{j2\pi \frac{i}{M} n} \end{aligned} \quad (14)$$

In [15] an efficient implementation of FMT using IFFT/ FFT is derived by introducing the polyphase components of the filter causing the filtering to be performed at a rate $1/T$ instead of M/T. In FMT the filters are not designed to satisfy the PR condition. Hence, while the system is robust against ICI, it will introduce ISI in each subcarrier. Equalization can be performed in the time or frequency domain using a per-subcarrier MMSE based DFE [15].

III. UNDERWATER ACOUSTIC CHANNEL

Depending on the type of channel configuration, factors that characterize the UWA propagation include transmission loss, propagation delay, ambient noise, multipath propagation and Doppler spread. Transmission loss depends on both distance and frequency. It is mainly caused by geometrical spreading, scattering and absorption. High frequency acoustic signals are attenuated to a larger extent compared to low frequency signals

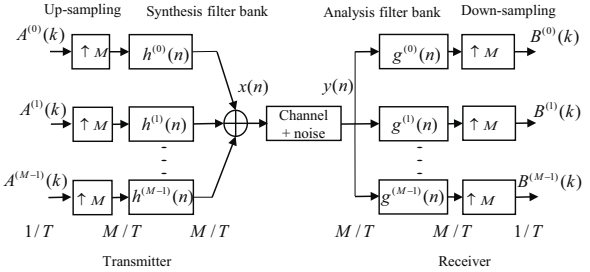

Fig. 3. Filtered Multitone (FMT) transceiver block diagram

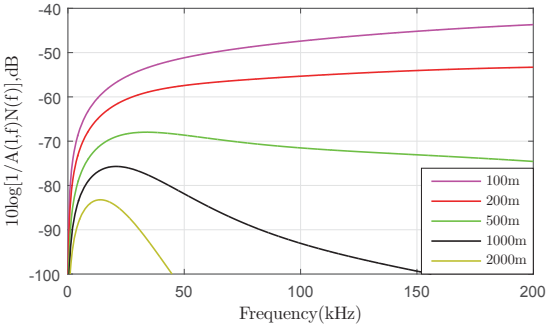

Fig. 4. Graph showing dependence of SNR on frequency and distance

for a given distance. The transmission loss (in dB) is often written as [1]

$$10\log A(l,f) = k.10\log l + l.10\log \alpha(f) \tag{15}$$

where $\alpha(f)$ represents the absorption coefficient in dB/km, l is the transmission distance in meters, k represents the geometrical spreading factor which takes values between 1 and 2 for cylindrical and spherical spreading respectively. $\alpha(f)$ can be computed in dB/km using a simple model known as the Thorp Model which only depends on the frequency and is given by:

$$10\log\alpha(f)=\frac{0.11f^2}{1+f^2}+\frac{44f^2}{4100+f^2}+2.75\times10^{-4}f^2+0.003 \tag{16}$$

A more accurate model known as the Fisher and Simmons model can be used to calculate the absorption coefficient (used in the simulations). This model considers the effects of temperature, pressure, salinity and relaxation frequencies due to the chemical components, namely boric acid and magnesium sulphate, and is valid for the frequency range of 100 Hz $<f<$1 MHz [16].

The low speed of sound in water induces a high propagation delay that significantly affects the throughput of the system. The speed of sound in water is dependent on the depth, temperature, and salinity of seawater and is expressed as [16]

$$\begin{aligned} c=&1448.96+4.591T-0.05304T^2+0.0002374T^3\\ &+1.340(S-35)+0.0163z+1.675\times10^{-7}z^2\\ &-0.01025T(S-35)-7.139\times10^{-13}Tz^3 \end{aligned} \tag{17}$$

Equation (17) is applicable for a temperature (T) range between 0 and 30, in degrees Celcius, salinity (S) range between 30 and 40 parts per million (ppm) and depth (z) between 0 and 8000 m. This model adequately defines the sound velocity profile and hence can be used for propagation delay modelling.

Ambient noise sources include turbulence, breaking waves, distant shipping and thermal noise. These are defined by the Empirical formulae (in dB re μPa per Hz where frequency is in kHz) [1]:

$$\begin{aligned} 10\log N_t(f)&=17-30\log(f)\\ 10\log N_s(f)&=40+20(s-0.5)+26\log(f)-60\log(f+0.03)\\ 10\log N_w(f)&=50+7.5w^{0.5}+20\log(f)-40\log(f+0.4)\\ 10\log N_{th}(f)&=-15+20\log(f) \end{aligned} \tag{18}$$

where N_t represents the turbulence noise, N_s is the shipping noise (s is known as the shipping factor and takes a value between 0 and 1), N_w is the noise due to breaking waves as a result of wind (w represents the speed of wind in m/s) and N_{th} is the thermal noise. The overall power spectral density (PSD) of the ambient noise is expressed as (in μ Pa) [1]:

$$N(f)=N_t(f)+N_s(f)+N_w(f)+N_{th}(f) \tag{19}$$

The narrowband SNR can be derived by considering the transmission loss for a distance l and frequency f, average transmitted signal power P and the spectrum of the ambient noise $N(f)$. The expression (in μPa re dB per Hz) is [1]

$$SNR(l,f)=\frac{P/A(l,f)}{N(f)\Delta(f)}=\frac{S(f)}{N(f)A(l,f)} \tag{20}$$

where $\Delta(f)$ is the bandwidth of the receiver noise and $S(f)$ is the PSD of the transmitted signal. There is an optimum frequency for each transmitter-receiver separation at which maximum narrowband SNR is achieved at the receiver. A graph of the inverse of the AN product is shown in Fig. 4 for various transmitter-receiver separation. For multipath propagation, the frequency response of the pth path is given by:

$$H_p(f)=\Gamma_p/\sqrt{A(l_p,f)} \tag{21}$$

where l_p is the length of the pth propagation path with an associated delay of $\tau_p=(l_p/c)-t_0$ (c is the speed of sound in water and t_0 denotes a reference time at the receiver), Γ_p is the cumulative reflection coefficient for surface and bottom reflections. The overall channel response in the frequency domain is [17]

$$H(f)=\sum_p H_p(f)e^{-j2\pi f\tau_p} \tag{22}$$

and the corresponding impulse response is given by

$$h(t)=\sum_p h_p(t-\tau_p) \tag{23}$$

where $h_p(t)$ is the IFFT of $H_p(f)$. A baseband model of the UWA channel with discrete multipath components can be represented as follows [1]

$$c(\tau,t)=\sum_p A_p(t)\delta(\tau-\tau_p(t)) \tag{24}$$

where A_p and τ_p represent the time-varying paths amplitudes and delays respectively. For a given data block, a Doppler scale factor can be applied to each path delay as follows [1]

$$\tau_p(t)=\tau_p-a_pt \tag{25}$$

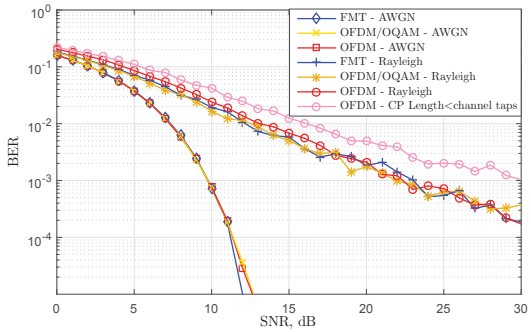

Fig. 5. BER performance of OFDM and FBMC in AWGN and 5-tap Rayleigh fading channels

For N_p dominant discrete paths, the UWA channel model can be expressed as follows [1]

$$c(\tau,t)=\sum_{p=1}^{N_p} A_p \delta(\tau-[\tau_p-a_p t]) \tag{26}$$

IV. Simulation Results

Fig. 5 shows the BER performance for un-coded OFDM and FBMC (FMT and OFDM-OQAM) systems in AWGN channel and a 5-tap Rayleigh fading channel. QPSK modulation and 8192 subcarriers were used for both OFDM and FBMC systems. The prototype filter for the OFDM-OQAM system is based on (10) with an overlapping factor of $K=4$ while the prototype filter for the FMT system is a FIR Hamming filter with an overlapping factor of $\gamma=10$. It was assumed that the receiver has perfect channel knowledge and each subcarrier experiences only flat fading in the Rayleigh channel scenario. Hence a single-tap equalizer was used for all systems where the received signal on each subcarrier was divided by the frequency domain channel response to yield the estimated symbols. As can be observed from the plots, FBMC systems provide similar performance as their OFDM counterpart both under AWGN and multipath fading channels. FBMC systems do not require a CP but can still provide the same performance as CP-OFDM. Hence for similar system parameters, FBMC systems provide higher bit rate which is very much desirable for underwater video transmission. The prototype filter in FMT is usually designed to have a sharp cut-off in the frequency domain. As a result the filters will be longer and have larger sidelobes in the time domain. So even in an ideal channel scenario ISI is likely to occur and per sub-channel adaptive equalization will be required to cancel the interference. On the other hand because in OFDM-OQAM each subcarrier is modulated with a real-valued symbol instead of complex, pulse shape filters with good time-frequency localisation can be used (such as IOTA filter). These reduce both ISI and ICI without the addition of any CP [18]. It should be noted however that according to Balian Low Theorem, for a multicarrier system we cannot simultaneously achieve the three desirable features of a filter which is well localized in time and frequency, has maximum spectrum efficiency and perfect orthogonality. So there needs to be a trade-off between orthogonality and time-frequency localization so as to achieve maximum throughput

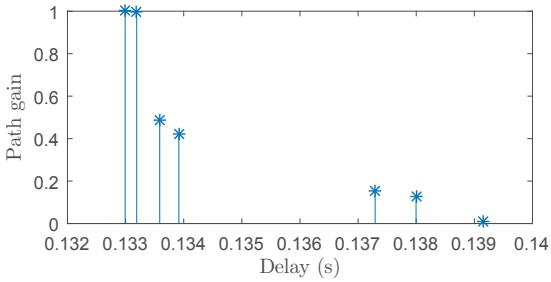

Fig. 6. UWA impulse response for horizontally configured channel

in a given channel realization [19]. Table I shows the spectral efficiency of OFDM, FMT [7] and OFDM-OQAM where T is the symbol period, T_{CP} is the OFDM cyclic prefix duration and α is the roll-off factor of the prototype filter in FMT.

TABLE I
SPECTRAL EFFICIENCY OF MULTICARRIER SYSTEMS

Multicarrier System	Symbol Period	Subcarrier Spacing	Spectral Efficiency
CP-OFDM	$T+T_{CP}$	$1/T$	$T/(T+T_{CP})$
OFDM-OQAM	T	$1/T$	1
FMT	T	$(1+\alpha)/T$	$1/(1+\alpha)$

Since OFDM-OQAM achieves the maximum bandwidth efficiency (100%), it is a very good candidate for UWA video transmission and hence it will be considered for the following UWA channel simulation instead of FMT. Two UWA transmission scenarios are examined: a horizontally configured one and a vertically configured one.

For a shallow water horizontally configured multipath channel, the transmitter and receiver are assumed to be submerged at a depth of 20 m and 2 m respectively (water depth = 25 m). They are separated by a horizontal distance of 200 m. The frequency ranges from 40 kHz to 155 kHz with a center frequency of 97.5 kHz. The maximum delay spread in this scenario is 6.1 ms. The CIR for this channel scenario is shown in Fig. 6.

As for the vertical transmission scenario, the transmitter-receiver pair are submerged at a depth of 195 m and 2 m respectively (water depth of 200 m). In this type of channel configuration, the multipath effect is more relaxed and hence the achievable bit rate is only limited by the available bandwidth [20]. Hence in this case we have considered only a single-path transmission which suffers only from a delay and attenuation over the vertical transmission distance.

Fig. 7 shows the BER performance of OFDM and OFDM-OQAM (referred to as FBMC) in both channel scenarios. For the purpose of simulation, 16-QAM modulation was used with the number of subcarriers set at 8192. "HCC" refers to a shallow water horizontally configured multipath channel while "VCC" refers to a vertically configured channel. Reed Solomon (RS) and Turbo codes are used for error correction. It is to be noted that Doppler Effect has not been considered in this case. CP-OFDM and OFDM-OQAM yield similar performance in both channels. For a similar code rate, Turbo codes with 8 iterations greatly outperform RS codes. For instance at a BER of 10^{-3}, Turbo-coded FBMC outperforms RS-coded FBMC by 9.7 dB in a vertically configured channel and 5.2

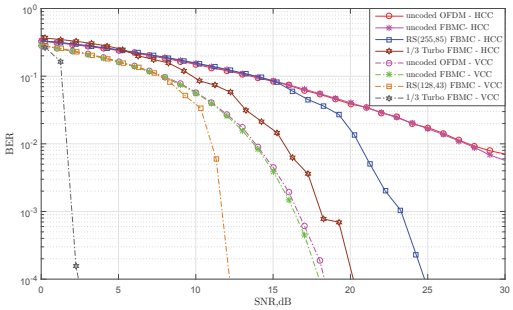

Fig. 7. BER performance of OFDM and OFDM-OQAM systems in UWA channels

dB in a horizontally configured multipath UWA channel. Note that usually the minimum number of subcarriers in an OFDM system depends on the RMS delay spread in the channel. In [2] the number of subcarriers that has been found to be appropriate was between 8192 and 16384 for the same bandwidth, carrier frequency and transmission distance. The useful bit rate of an OFDM system can be computed as

$$bitrate{=}r{\times}\frac{M}{T{+}T_{CP}}{\times}no.\quad of\quad bits/symbol \tag{27}$$

where r is the FEC code rate, M is the number of subcarriers, T is the OFDM symbol duration and T_{CP} is the guard interval.

Assuming 8192 subcarriers and a CP duration of 10 ms for OFDM, a code rate of 0.3 and 16-QAM modulation, the theoretical bit rates for OFDM and OFDM-OQAM systems are given in Table II.

TABLE II
THEORETICAL ACHIEVABLE BIT RATE

	Symbol Period (ms)	Band-width (kHz)	No. of subcar-riers	Bandwidth Efficiency (sps/Hz)	Bi-trate (kbps)
CP-OFDM	81.2	115	8192	0.88	121
OFDM-OQAM	71.2	115	8192	1	138

For the vertical acoustic channel scenario, FEC codes with higher code rate can be used together with higher modulation schemes in order to achieve a much better bit rate since the number of errors in this channel is more relaxed. However for video transmission, the number of errors should be kept as low as possible since a single bit error can cause a whole video packet to be discarded, thus degrading video quality.

V. Conclusion

OFDM is a very popular technique that has been used over the years for terrestrial wireless communication as well as UWA communication. However it has some drawbacks which question its usage for future generation wireless networks where higher data rates are desirable. In this paper we have shown that FBMC systems can provide the same performance as the traditional OFDM in AWGN, Rayleigh and UWA channels without the use of a cyclic prefix. This makes FBMC (especially OFDM-OQAM) attractive for UWA video transmission where high data rates are very desirable for delivering good quality video given the very limited acoustic bandwidth. We have also shown that with the use of powerful codes such as Turbo codes, very good BER performance is obtained in UWA channels. It should be noted however that FBMC systems have higher complexity in terms of implementation and equalization at the receiver.

References

[1] H. Esmaiel, D. Jiang *et al.*, "Review article: multicarrier communication for underwater acoustic channel," *Int'l J. of Communications, Network and System Sciences*, vol. 6, no. 08, p. 361, 2013.

[2] J. Ribas, D. Sura, and M. Stojanovic, "Underwater wireless video transmission for supervisory control and inspection using acoustic OFDM," in *OCEANS 2010*, Sep. 2010, pp. 1–9.

[3] L. D. Vall, D. Sura, and M. Stojanovic, "Towards underwater video transmission," in *Proceedings of the Sixth ACM International Workshop on Underwater Networks*. ACM, 2011, p. 4.

[4] R. Ahmed, L. D. Vall, M. Stojanovic, and R. Narayanaswami, "Video transmission over an in-air acoustic link," *In Proc. Workshop on Underwater Networks (WUWNet)*, Dec. 2011.

[5] M. Alard, "Construction of a multicarrier signal," Aug. 21 2001, uS Patent 6,278,686.

[6] R. Haas and J.-C. Belfiore, "A time-frequency well-localized pulse for multiple carrier transmission," *Wireless personal communications*, vol. 5, no. 1, pp. 1–18, 1997.

[7] J. Gomes and M. Stojanovic, "Performance analysis of filtered multitone modulation systems for underwater communication," in *OCEANS 2009, MTS/IEEE Biloxi-Marine Technology for Our Future: Global and Local Challenges*. IEEE, 2009, pp. 1–9.

[8] P. Amini, R.-R. Chen, and B. Farhang-Boroujeny, "Filterbank multicarrier communications for underwater acoustic channels," *Oceanic Engineering, IEEE Journal of*, vol. 40, no. 1, pp. 115–130, 2015.

[9] A. Aminjavaheri, A. RezazadehReyhani, and B. Farhang-Boroujeny, "Frequency spreading Doppler scaling compensation in underwater acoustic multicarrier communications," in *Communications (ICC), 2015 IEEE International Conference on*, Jun. 2015, pp. 2774–2779.

[10] Q. He and A. Schmeink, "Comparison and evaluation between FBMC and OFDM systems," in *WSA 2015; 19th International ITG Workshop on Smart Antennas; Proceedings of*, Mar. 2015, pp. 1–7.

[11] M. Bellanger, D. Le Ruyet, D. Roviras, M. Terré, J. Nossek, L. Baltar, Q. Bai, D. Waldhauser, M. Renfors, T. Ihalainen *et al.*, "FBMC physical layer: a primer," *PHYDYAS, January*, 2010.

[12] M. Aldababseh and A. Jamoos, "Estimation of FBMC/OQAM fading channels using dual Kalman filters," *The Scientific World Journal*, vol. 2014, 2014.

[13] A. Viholainen, M. Bellanger, and M. Huchard, "Prototype filter and structure optimization," *website: www. ict-phydyas. org: Document D*, vol. 5, 2009.

[14] J. Louveaux, L. Baltar, D. Waldhauser, M. Renfors, M. Tanda, C. Bader, and E. Kofidis, "Equalization and demodulation in the receiver (single antenna)," *ICT-211887 PHYDYAS deliverable D*, vol. 3, 2008.

[15] I. Berenguer and I. J. Wassell, "FMT modulation: receiver filter bank definition for the derivation of an efficient implementation," in *Proc. 7th International OFDM Workshop*, 2002, pp. 158–162.

[16] M. C. Domingo, "Overview of channel models for underwater wireless communication networks," *Physical Communication*, vol. 1, no. 3, pp. 163–182, 2008.

[17] M. Stojanovic, "Underwater acoustic communications: Design considerations on the physical layer," in *Wireless on Demand Network Systems and Services, 2008. WONS 2008. Fifth Annual Conference on*. IEEE, 2008, pp. 1–10.

[18] J. Du and S. Signell, "Classic OFDM systems and pulse shaping OFDM/OQAM systems," 2007.

[19] H. Bolcskei, P. Duhamel, and R. Hleiss, "Design of pulse shaping OFDM/OQAM systems for high data-rate transmission over wireless channels," in *Communications, 1999. ICC '99. 1999 IEEE International Conference on*, vol. 1, 1999, pp. 559–564 vol.1.

[20] C. Pelekanakis, M. Stojanovic, and L. Freitag, "High rate acoustic link for underwater video transmission," in *OCEANS 2003. Proceedings*, vol. 2, Sep. 2003, pp. 1091–1097 Vol.2.